Unconventional Vortex States in Nanoscale Superconductors Due to Shape-Induced Resonances in the Inhomogeneous Cooper-pair Condensate

L.-F. Zhang, L. Covaci, M. V. Milošević, G. R. Berdiyorov, and F. M. Peeters*

Departement Fysica, Universiteit Antwerpen, Groenenborgerlaan 171, B-2020 Antwerpen, Belgium

(Received 9 May 2012; published 4 September 2012)

Vortex matter in mesoscopic superconductors is known to be strongly affected by the geometry of the sample. Here we show that in nanoscale superconductors with coherence length comparable to the Fermi wavelength the shape resonances of the order parameter results in an additional contribution to the quantum topological confinement—leading to unconventional vortex configurations. Our Bogoliubov–de Gennes calculations in a square geometry reveal a plethora of asymmetric, giant multivortex, and vortex–antivortex structures, stable over a wide range of parameters and which are very different from those predicted by the Ginzburg–Landau theory. These unconventional states are relevant for high-T_c nanograins, confined Bose–Einstein condensates, and graphene flakes with proximity-induced superconductivity.

DOI: 10.1103/PhysRevLett.109.107001 PACS numbers: 74.78.Na, 74.25.Ha, 74.25.Uv, 74.45.+c

In the last decades, the effect of the boundary on mesoscopic superconductors with dimensions comparable to the penetration depth λ or the coherence length ξ has been intensively studied [1–8]. In an applied magnetic field, it was found that the vortex states strongly depend on the size and geometry of the sample and are generally different from the Abrikosov triangular lattice observed in bulk type-II conventional superconductors (where only the vortex–vortex interaction plays a role). For example, a giant vortex induced by strong boundary confinement was predicted [2] as the ground state in disks which was subsequently observed experimentally [9,10]. In square samples, a peculiar state with an antivortex at the center surrounded by four vortices was predicted theoretically [11,12], but never observed experimentally up to now.

All of the above theoretical works are based on the Ginzburg–Landau (GL) theory. When the superconductor is downscaled to nanometer sizes, quantum confinement [13] leads to unique phenomena, especially in samples with dimensions of the order of the Fermi wave length λ_F. The GL theory is no longer applicable in this regime and the microscopic Bogoliubov–de Gennes (BdG) formalism is required. The discretization of the energy levels around the Fermi level E_F was shown to induce quantum-size effect [14,15], quantum-size cascades [16], and the shell effect [17]. As one of the important results, Ref. [15] reported the wavelike inhomogeneous spatial distribution of the order parameter, further enhanced at the boundary due to quantum confinement. The latter is important because it is well known that vortices tend to migrate and be pinned in areas where superconductivity is suppressed [18], i.e., it is energetically favorable for a vortex to suppress the superconducting order parameter in the region where it is already weak. In reality, the behavior is much more complex and in some instances the vortex can be pinned where the gap is large [19]. The appearance of oscillations in the order parameter profile due to quantum confinement is thus expected to influence the vortex states. For conventional superconductors, $k_F\xi_0 \approx 10^3$ (k_F is the Fermi wave vector and ξ_0 is the BCS coherence length), systems of size comparable to λ_F will not be large enough to host a vortex (being much smaller than the coherence length). However, materials with small coherence lengths, e.g., high-T_c cuprate superconductors, will have $k_F\xi_0 \approx 1$–4 and therefore in such systems it is possible to obtain vortex states in the quantum confinement regime. Another such system is a graphene flake deposited on top of a superconductor. Because of the proximity effect, superconducting correlations will diffuse in graphene [20–23]. Such a system is in the clean limit because the scattering length in graphene is large. More importantly, in graphene, near the Dirac point, the Fermi wavelength is very large and can be easily manipulated by doping. In other words, $k_F\xi_0$ can be tuned, which will allow for different vortex patterns to be realized in the graphene flake in the quantum confinement regime, but for more accessible sample sizes (above 100 nm).

In order to experimentally detect vortex states in nanosized superconductors, one can extract information about the local density of states (LDOS) from measurements of the differential conductance with scanning tunneling microscopy [10,24,25]. An extensive analysis of the LDOS profile of the vortex states has been performed in the past [26–30]. It is generally known that the bound states in the vortex core lead to peaks in the LDOS at energies below the superconducting gap, though the exact formation of peaks in the spectrum of a multiple flux line (giant vortex) will depend on the vorticity [31]. Also, when $k_F\xi_0$ is small, the spectrum becomes particle-hole asymmetric and the lowest vortex bound state has a finite energy [26]. In the quantum confinement regime, there exist strong vortex–vortex and vortex–boundary interactions and the quasiparticle spectrum becomes much more complicated. In this case, the lowest bound state peak position does not generally coincide with the vortex core [32]. Furthermore, in case of strong interactions, vortex and surface bound states may combine to form

a complex state where LDOS contributions of individual constituents are not clearly visible.

In this Letter, we report novel vortex states that appear from the interplay between quantum confinement, inhomogeneous superconductivity, an external magnetic field, and the sample geometry, in a nano-sized superconducting square. We performed calculations for a sample in the quantum limit by solving BdG equations self-consistently. In what follows, we keep constant the size of the sample and the bulk coherence length $\xi_0 = \hbar v_F/\pi\Delta_0$ (where v_F is the Fermi velocity and Δ_0 is the order parameter at zero temperature), while we change the parameter $k_F\xi_0$ and thereby tune the influence of the confinement on the vortex structure. We start from the well-known BdG equations:

$$[K_0 - E_F]u_n(\vec{r}) + \Delta(\vec{r})v_n(\vec{r}) = E_n u_n(\vec{r}), \quad (1)$$

$$\Delta(\vec{r})^* u_n(\vec{r}) - [K_0^* - E_F]v_n(\vec{r}) = E_n v_n(\vec{r}), \quad (2)$$

where $K_0 = (i\hbar\nabla + e\vec{A}/c)^2/2m$ is the kinetic energy and E_F is the Fermi energy, $u_n(v_n)$ are electron- (hole) like quasiparticle eigen wave functions, E_n are the quasiparticle eigen energies, and $\vec{A}$ is the vector potential (we use the gauge $\nabla \cdot \vec{A} = 0$).

The pair potential is determined self-consistently from the eigen wave functions and eigen energies:

$$\Delta(\vec{r}) = g \sum_{E_n<E_c} u_n(\vec{r})v_n^*(\vec{r})[1 - 2f_n], \quad (3)$$

where g is the coupling constant, E_c is the cutoff energy, and $f_n = [1 + \exp(E_n/k_BT)]^{-1}$ is the Fermi distribution function, where T is the temperature. We consider the two-dimensional problem and assume a circular Fermi surface. The confinement imposes Dirichlet boundary conditions [i.e., $u_n(\vec{r}) = 0$, $v_n(\vec{r}) = 0$, $r \in \partial S$] such that the order parameter vanishes at the surface. In an extreme type-II superconductor (and/or very thin sample), it is reasonable to neglect the contribution of the supercurrent to the total magnetic field. For such a case, we discretize Eqs. (1)–(3) and by using the finite difference method we solve them self-consistently.

The free energy [33,34] of the system is then calculated as:

$$F = \sum_n 2E_n f_n + k_BT[f_n \ln f_n + (1 - f_n)\ln(1 - f_n)] + \int d\vec{r}\Big[-2\sum_n E_n|v_n|^2 + 2\Delta(\vec{r})\sum_n u_n^* v_n[1 - 2f_n] - g\sum_n u_n^* v_n(1 - 2f_n)\sum_{n'} u_{n'} v_{n'}^*(1 - 2f_{n'})\Big], \quad (4)$$

where the spatial dependence of u_n and v_n is implicit. The LDOS $N(r, E)$ is calculated from

$$N(r, E) = -\sum_n [f'(E_n - E)|u_n|^2 + f'(E_n + E)|v_n|^2]. \quad (5)$$

In this Letter, we consider as an example a thin superconducting square with size $5\xi_0 \times 5\xi_0$. The microscopic parameters are set to keep $\Delta_0/E_c = 0.2$. The calculations are done for different parameters $k_F\xi_0$. Because we consider the zero temperature case, the system is always in the quantum limit (where $T < 1/k_F\xi_0$). Figure 1 shows our numerical results for the free energy of the found stable vortex configurations (the states with up to five vortices are shown) for two values of the key parameter, $k_F\xi_0$. The insets show the inhomogeneous profile of the superconducting order parameter in the absence of an applied magnetic field which is expected to strongly influence the vortex structure. When comparing with conventional free energy curves obtained from the GL theory [35], many differences can be observed. First, the penetration field for the first vortex is suppressed because the order parameter is not homogeneous, allowing the vortex to penetrate easier at locations where the order parameter is weakened. Second, the stability range in flux for different vortex states (with vorticity L) is not monotonically decreasing towards $1\Phi_0$ as L increases. Moreover, those stability ranges strongly vary when $k_F\xi_0$ is changed. For example, for $k_F\xi_0 = 2$ the vortex structures with even vorticity are stable over a broader magnetic field range, while for $k_F\xi_0 = 3$ surprisingly the structures with odd vorticity are the favored ones. The main reason behind this phenomenon is that different confinement-induced oscillations in the order parameter

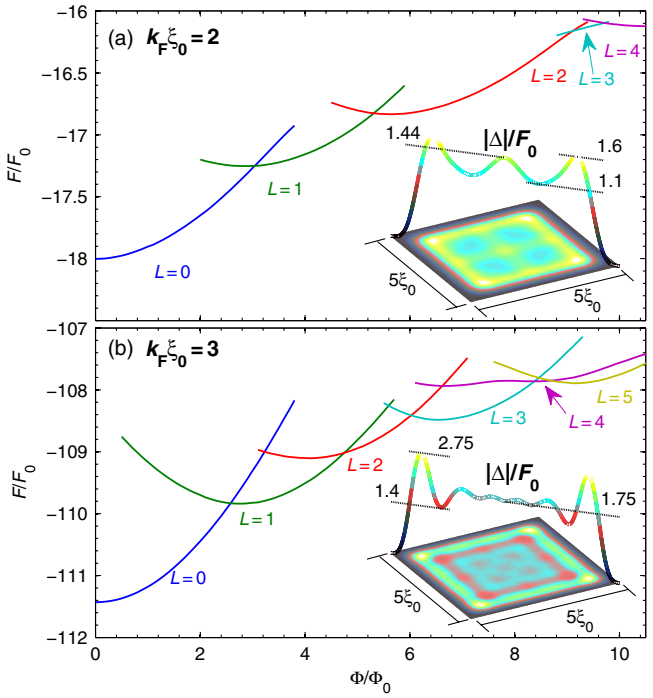

FIG. 1 (color online). Free energy as a function of the magnetic flux through the square sample, for (a) $k_F\xi_0 = 2$ and (b) $k_F\xi_0 = 3$. Here, $F_0 = \hbar^2/2m\xi_0^2$. The insets show the contour plots of the order parameter with the diagonal profiles in the absence of applied magnetic field.

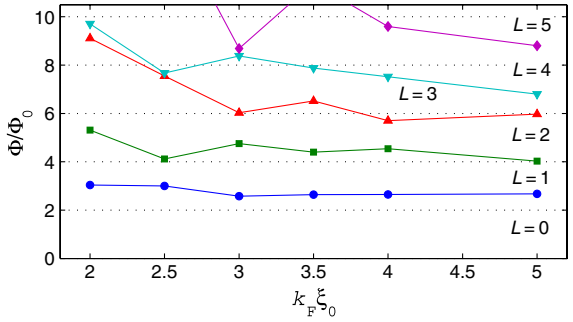

FIG. 2 (color online). Transition fluxes in units of Φ_0 between ground states with consecutive vorticities for different $k_F\xi_0$.

for different $k_F\xi_0$ value will stabilize different symmetries of the vortex pattern. To illustrate this effect better, we plot in Fig. 2 the applied magnetic flux at which ground state transitions between states with consecutive vorticities occur, as a function of $k_F\xi_0$. Notice the varying ranges of stability of different vortex states, which are very sensitive to $k_F\xi_0$. Of course, for large $k_F\xi_0$ the behavior of the system converges to a more conventional picture (with each new vortex entering the system with roughly one flux-quantum added).

To underpin the reasons for this varying stability of vortex states in what is otherwise a rather simple, square system, we show in Fig. 3 some of the typical states for the case of $k_F\xi_0 = 2$ (the order parameter, its phase, and corresponding LDOS). As elaborated above, the quantum confinement of electrons here strongly affects the spatial distribution of the order parameter [see inset in Fig. 1(a)], having three o scillations across the square and four distinct minima that enhance the fourfold symmetry. This automatically leads to

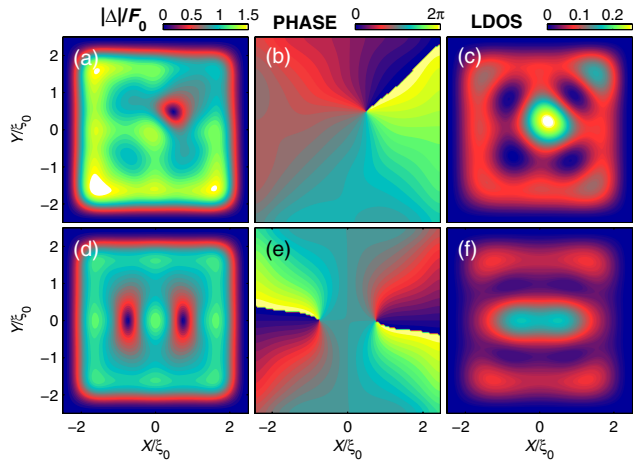

FIG. 3 (color online). Contour plots of the absolute value of the order parameter (left), the phase of the order parameter (center), and the LDOS at $E/F_0 = 0.57$ in (c) and $E/F_0 = 0.48$ in (f) (right) for $k_F\xi_0 = 2$. Panels (a), (b), and (c) are for $\Phi/\Phi_0 = 4$ and $L = 1$ state. Panels (d), (e), and (f) correspond to $\Phi/\Phi_0 = 6$ and $L = 2$ state.

the improved stability of states with even vorticity, similar to the case of a square with four antidots [36]. We also observe that, before ceasing at the boundary, the order parameter is enhanced near the surface, with the highest value found near the corners. Because of the effect of the boundary and the shape resonances, the order parameter is also enhanced at the center of the square. To reiterate a fairly obvious point, vortices are repelled by the peak positions of the superconducting pair amplitude, and the four low amplitude locations (with value only 2/3 of the peaks) will pin vortices rather strongly. Figures 3(a)–3(c), show the $L = 1$ ground state for applied flux $\Phi/\Phi_0 = 4$. Surprisingly, we find that the only vortex in this state is actually sitting in one of the minima of the order parameter and the fourfold symmetry is broken. We emphasize that this state is not possible within the GL formalism where the single vortex will always sit in the center of the square.

From an experimental point of view, in the absence of any reference energy, the zero-bias LDOS is most relevant. Here instead we will show the LDOS for the lowest energy vortex bound state, which for an isolated vortex could be found from a simple empirical formula $E_{\text{low}}/\Delta = (2k_F\xi_0)^{-1}\ln(3.33k_F\xi_0)$ [26]. Therefore, for the $L = 1$ state we plot the LDOS at $E/F_0 = 0.57$ [Fig. 3(c)]. Note that this lowest vortex bound state is not localized in the vortex core but is shifted towards the center of the square. We attribute this to the interactions of the quasiparticles not only with the four deepest minima of the inhomogeneous order parameter but also with the edges and the corners—where the order parameter is also suppressed [see inset of Fig. 1(a)]. The effect of this interaction can also be inferred from the finite LDOS at the corner of the sample, next to the vortex.

When increasing the magnetic field further, an additional vortex enters the system (forming $L = 2$ state) and another unexpected spatial distribution is stabilized. We illustrate this in Figs. 3(d)–3(f) for applied flux $\Phi/\Phi_0 = 6$. The confinement seems to act strongly and vortices are compressed closer to each other. However, the enhancement of the order parameter in the center of the sample due to quantum resonance prevents the two vortices from merging. As a consequence, vortices are squeezed into elliptical shapes, as a pair parallel to one of the sample edges. This vortex configuration is as different as one can be from the known GL results, where the two vortices are always found sitting on the diagonal, or merged into a giant vortex, and have always an almost circular core. The LDOS plot [Fig. 3(f)] again reveals strong competing interactions, different from those acting on vortices. For example, we see evidence of the interaction of bound states inside the vortex cores, because the maximum in the LDOS is reached between the vortices and not at the center of each vortex. Also, the vortex—surface interaction of the bound states is enhanced, leading to LDOS being clearly appreciable near the surface.

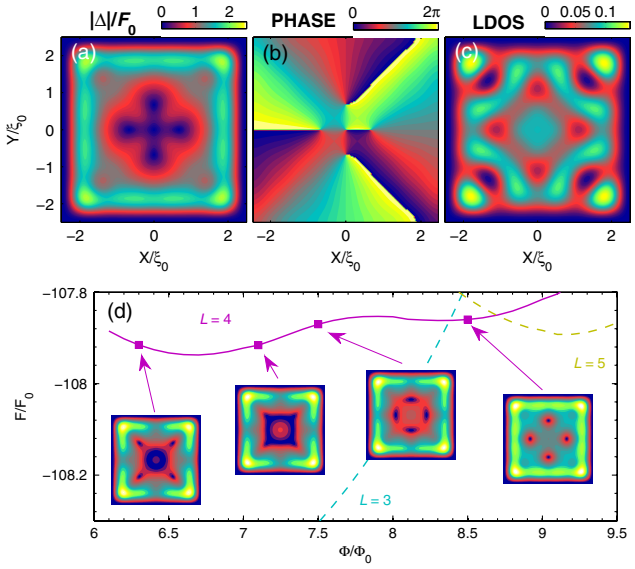

FIG. 4 (color online). Contour plots of the absolute value of the order parameter (a), the phase of the order parameter (b), and the LDOS at $E/F_0 = 0.57$ in (c) for $k_F\xi_0 = 3$ and $\Phi/\Phi_0 = 7$ ($L = 3$). Panel (d) shows the vortex configurations for the $L = 4$ state and their corresponding energies.

To check further the influence of the length scales in our sample, we also calculated the vortex states for $k_F\xi_0 = 3$. In this case, the inset of Fig. 1(b) shows six local maxima along the diagonal, twice as many as in the $k_F\xi_0 = 2$ case. There are also strong oscillations near the corners but relatively flatter away from the boundary. Again, as expected, the fourfold symmetry is maintained, but now there are no strong minima in the fourfold arrangement deep inside the sample. For that reason, for $\Phi/\Phi_0 = 3$, the $L = 1$ ground state is conventional and contains one vortex at the center of the square. For $\Phi/\Phi_0 = 5.8$, the $L = 2$ state is the ground state and although it still shows the vortex pair parallel to the side of the square, the shape of the vortices and the location of the lowest bound state LDOS peaks bring it closer to the conventional picture [37].

However, when the flux through the square is increased to $\Phi/\Phi_0 = 7$, as shown in Figs. 4(a)–4(c), the ground state has vorticity $L = 3$ and is not conventional. We in fact find the vortex–antivortex (v–av) molecule, similar to the symmetry-induced ones predicted by the GL theory [11,12] (four vortices with an antivortex in between, so that the total vorticity is $L = 4 - 1$). There the size of the v–av molecule was found to be very small, possibly larger if artificial pinning centers are introduced [12,38]. In the present case, the v–av molecule is stable over a wide range of fields because of the symmetry of the oscillatory pattern of the order parameter due to the quantum confinement. The LDOS at $E/F_0 = 0.57$, shown in Fig. 4(c), reveals again that because the vortices are located closer together, the bound states are not localized in the cores but are extended over the whole square.

Another found difference from earlier studies is the behavior of the $L = 4$ state for $k_F\xi_0 = 3$. As shown in the free energy curve in Fig. 4(d), we revealed a continuous phase transition between the configuration with the vortices located on the diagonal (at lower fields) and the configuration with the four vortices sitting near the edges of the square (higher fields), a state never found within GL. The transition between the two fourfold symmetric states is quite peculiar and yet unseen in mesoscopic superconductivity—it involves the appearance of v–av pairs near the center of the square [39]. As the field is increased, the diagonal vortices annihilate with the central antivortices, and central vortices move to the side location. Moreover, the $L = 4$ configuration with side vortices becomes the ground state for $\Phi/\Phi_0 = 8.5$. Because of the inhomogeneity of the order parameter, these vortices never merge into a giant vortex, contrary to the known GL picture for samples of smaller sizes.

In conclusion, we found novel vortex states with unconventional stability ranges and unconventional transition between them in a superconducting square in the quantum limit, where significant departures from previous works based on the GL theory are found. Experimentally, these states can be accessed through scanning tunneling microscopy measurements. Additionally, we showed that competing interactions in the quantum limit for the bound states are different from those for the vortices, so that the conventional picture of a vortex bound to lowest energy states does not hold. Instead we predict that the maxima in LDOS of the lowest energy states will be observed between vortices and near surfaces. These peculiar phenomena are made possible by strong quantum confinement, which induces spatial oscillations in the order parameter. Their specific pattern depends on the ratio of ξ_0 and λ_F, which is unfavorable for oscillations in elementary superconductors, but is small enough in high-T_c materials. However, to observe these novel states in the latter case, one should deal with very small samples. As an alternative, we propose the study of a graphene flake in contact to a superconducting film, where the Fermi energy of graphene can be tuned by a gate. In the case of graphene on Pb, our calculations show that one could tune $k_F\xi_0$ in the broad range of 0.1–10 by shifting the Fermi energy in a 400 × 400 nm flake from 0.01 to 0.1 eV above the Dirac point. Another system where effects of quantum confinement on vortex matter can be probed systematically are the optically trapped cold gases [40], which are nowadays extremely controllable. Further investigations will address the rich physics in the quantum limit, and show the effects of our findings in the 3D-confined case [41–43] and multicondensate samples [44], but where also barriers for vortex motion across the oscillating landscape can be investigated for possible use as Q bits or other vortex devices [45].

This work was supported by the Flemish Science Foundation (FWO-Vlaanderen).

*francois.peeters@ua.ac.be

[1] A. K. Geim, I. V. Grigorieva, S. V. Dubonos, J. G. S. Lok, J. C. Maan, A. E. Filippov, and F. M. Peeters, Nature (London) **390**, 259 (1997).

[2] V. A. Schweigert, F. M. Peeters, and P. S. Deo, Phys. Rev. Lett. **81**, 2783 (1998).

[3] J. J. Palacios, Phys. Rev. Lett. **84**, 1796 (2000).

[4] B. J. Baelus, F. M. Peeters, and V. A. Schweigert, Phys. Rev. B **63**, 144517 (2001).

[5] M. V. Milošević, S. V. Yampolskii, and F. M. Peeters, Phys. Rev. B **66**, 024515 (2002).

[6] C.-Y. Liu, G. R. Berdiyorov, and M. V. Milošević, Phys. Rev. B **83**, 104524 (2011).

[7] L. F. Chibotaru, A. Ceulemans, V. Bruyndoncx, and V. V. Moshchalkov, Phys. Rev. Lett. **86**, 1323 (2001).

[8] G. Teniers, L. F. Chibotaru, A. Ceulemans, and V. V. Moshchalkov, Europhys. Lett. **63**, 296 (2003).

[9] A. Kanda, B. J. Baelus, F. M. Peeters, K. Kadowaki, and Y. Ootuka, Phys. Rev. Lett. **93**, 257002 (2004).

[10] T. Cren, L. Serrier-Garcia, F. Debontridder, and D. Roditchev, Phys. Rev. Lett. **107**, 097202 (2011).

[11] L. F. Chibotaru, A. Ceulemans, V. Bruyndoncx, and V. V. Moshchalkov, Nature (London) **408**, 833 (2000).

[12] R. Geurts, M. V. Milošević, and F. M. Peeters, Phys. Rev. Lett. **97**, 137002 (2006); **75**, 184511 (2007).

[13] P. W. Anderson, J. Phys. Chem. Solids **11**, 26 (1959).

[14] A. A. Shanenko, M. D. Croitoru, and F. M. Peeters, Phys. Rev. B **75**, 014519 (2007).

[15] M. D. Croitoru, A. A. Shanenko, and F. M. Peeters, Phys. Rev. B **76**, 024511 (2007).

[16] A. A. Shanenko, M. D. Croitoru, and F. M. Peeters, Phys. Rev. B **78**, 024505 (2008).

[17] S. Bose, A. M. Garcia-Garcia, M. M. Ugeda, J. D. Urbina, C. H. Michaelis, I. Brihuega, and K. Kern, Nature Mater. **9**, 550 (2010).

[18] G. Blatter, M. V. Feigelman, V. B. Geshkenbein, A. I. Larkin, and V. M. Vinokur, Rev. Mod. Phys. **66**, 1125 (1994).

[19] D. Valdez-Balderas and D. Stroud, Phys. Rev. B **76**, 144506 (2007).

[20] H. B. Heersche, P. Jarillo-Herrero, J. B. Oostinga, L. M. K. Vandersypen, and A. F. Morpurgo, Nature (London) **446**, 56 (2007).

[21] H. Tomori, A. Kanda, H. Goto, S. Takana, Y. Ootuka, and K. Tsukagoshi, Physica (Amsterdam) **470C**, 1492 (2010).

[22] A. M. Black-Schaffer and S. Doniach, Phys. Rev. B **78**, 024504 (2008).

[23] L. Covaci and F. M. Peeters, Phys. Rev. B **84**, 241401 (2011).

[24] T. Nishio, T. An, A. Nomura, K. Miyachi, T. Eguchi, H. Sakata, S. Lin, N. Hayashi, N. Nakai, M. Machida, and Y. Hasegawa, Phys. Rev. Lett. **101**, 167001 (2008).

[25] T. Cren, D. Fokin, F. Debontridder, V. Dubost, and D. Roditchev, Phys. Rev. Lett. **102**, 127005 (2009).

[26] N. Hayashi, T. Isoshima, M. Ichioka, and K. Machida, Phys. Rev. Lett. **80**, 2921 (1998).

[27] S. M. M. Virtanen and M. M. Salomaa, Phys. Rev. B **60**, 14581 (1999).

[28] F. Gygi and M. Schluter, Phys. Rev. B **43**, 7609 (1991).

[29] A. S. Melnikov, D. A. Ryzhov, and M. A. Silaev, Phys. Rev. B **78**, 064513 (2008).

[30] C. Berthod, Phys. Rev. B **71**, 134513 (2005).

[31] B. Xu, M. V. Milošević, S.-H. Lin, F. M. Peeters, and B. Janko, Phys. Rev. Lett. **107**, 057002 (2011).

[32] A. S. Melnikov, D. A. Ryzhov, and M. A. Silaev, Phys. Rev. B **79**, 134521 (2009).

[33] I. Kosztin, S. Kos, M. Stone, and A. J. Leggett, Phys. Rev. B **58**, 9365 (1998).

[34] A. Spuntarelli, P. Pieri, and G. C. Strinati, Phys. Rep. **488**, 111 (2010).

[35] B. J. Baelus and F. M. Peeters, Phys. Rev. B **65**, 104515 (2002).

[36] G. R. Berdiyorov, B. J. Baelus, M. V. Milošević, and F. M. Peeters, Phys. Rev. B **68**, 174521 (2003).

[37] See Supplemental Material at http://link.aps.org/supplemental/10.1103/PhysRevLett.109.107001 for plots of the LDOS for vorticities $L = 1$ and $L = 2$ in the case when $k_F\xi_0 = 3$.

[38] R. Geurts, M. V. Milošević, and F. M. Peeters, Phys. Rev. B **79**, 174508 (2009).

[39] A movie containing plots of the order parameter and the current distribution as a function of applied field for the $L = 4$ state is provided as Supplemental Material at http://link.aps.org/supplemental/10.1103/PhysRevLett.109.107001.

[40] S. Aubin, S. Myrskog, M. H. T. Extavour, L. J. LeBlanc, D. McKay, A. Stummer, and J. H. Thywissen, Nature Phys. **2**, 384 (2006).

[41] B. Xu, M. V. Milošević, and F. M. Peeters, Phys. Rev. B **77**, 144509 (2008).

[42] M. M. Doria, A. R. de C. Romaguera, and F. M. Peeters, Phys. Rev. B **75**, 064505 (2007).

[43] M. A. Engbarth, S. J. Bending, and M. V. Milošević, Phys. Rev. B **83**, 224504 (2011).

[44] R. Geurts, M. V. Milošević, and F. M. Peeters, Phys. Rev. B **81**, 214514 (2010).

[45] M. V. Milošević, G. R. Berdiyorov, and F. M. Peeters, Appl. Phys. Lett. **91**, 212501 (2007).